Research Article

Pyrolysis, kinetics, and thermodynamic analysis of neem seed cake for the sustainable resource recovery

Manisha RANI[1]📍, **Rohan R. PANDE**[1]📍, **Kamalesh A. SORATE**[1,*]📍

[1]Department of Mechanical Engineering, Sardar Vallabhbhai National Institute of Technology, Surat, 394101, India

ARTICLE INFO

ABSTRACT

Pyrolysis has considerable potential for the monetization and management of neem seedcake by producing value-added compounds. The decomposition of neem seedcake (NSC) was analyzed, occurs in three stages: moisture removal (30–220°C), active decomposition (220–550°C), and slow char formation (550–800°C). The activation energies for seedcake pyrolysis were calculated using the Starink, Kissinger-Akahira-Sunose (KAS), and Ozawa-Flynn-Wall (OFW) methods, yielding values 235.985 kJ/mol, 235.918 kJ/mol, and 228.026 kJ/mol, respectively. The product exhibited highest activation energy 429.335 kJ/mol. The reaction rate increases exponentially as activation energy decreases. The isoconversional methods were used to predict activation energy of neem seedcake with coefficient of determination (R^2) greater than 0.90. The reaction chemistry of NSC pyrolysis, characterized by high reactivity, was evidenced by thermodynamic parameters (entropy, enthalpy and gibbs free energy), which indicated increasing endothermic behavior as rate of conversion (α) increased from 0.20 to 0.75. The positive change in enthalpy (230.92 kJ/mol) throughout the process indicates, when neem seedcake decomposes, energy is absorbed (endothermic behavior) to break the complex chemical bonds. The neem seedcake pyrolysis promotes sustainable waste management, reduces pollution, decreases reliance on fossil fuels, and supports climate change efforts. This study enhances knowledge of biomass pyrolysis, especially for less-explored non-edible oil seedcakes.

Cite this article as: Rani M, Pande RR, Soratet KA. Pyrolysis, kinetics, and thermodynamic analysis of neem seed cake for the sustainable resource recovery. J Ther Eng 2026;12(1):1–13.

INTRODUCTION

Global energy consumption is on a continuous upward trend, fueled by the economic development and growing populations of rapidly developing economies. Rapid urbanization, industrialization, and population growth are causing energy shortages and increasing environmental pollution. Rising demand depletes non-renewable resources and worsens pollution, highlighting the need for sustainable energy solutions [1,2]. In this context, biomass is coming to the fore as a renewable energy source due to its diverse applications. Agricultural residues, a part of lignocellulosic biomasses, have the potential to replace

*****Corresponding author.
*****E-mail address: kasorate@med.svnit.ac.in

fossil fuels for energy recovery and convert them into value-added products[3]. India's agroecological conditions make it ideal for cultivating a variety of oilseeds, such as soybean, groundnut, mustard, neem, and castor seeds[4-6]. According to Food and Agriculture Organization (FAO) of United Nations (UN), global oilseed production reached 628.54 million metric tons (MMT) in 2020. India contributed 50.69 MMT to this total, positioning it as one of the world's leading oilseed producers (FAO, 2020) [4]. Based on the latest available data, global oilseed production for the 2023-24 season is projected at approximately 626 million metric tons, with soybeans being the predominant crop, accounting for 398 million metric tons. India remains a significant contributor to oilseed production, particularly in soybeans, rapeseed, and peanuts. De-oiled cake, a by-product of oilseed extraction, produces around 650 grams of residue for every kilogram of seeds processed [6]. A large amount is utilized as animal feed, namely for fish and ruminants, because of their high protein content.

Many oil seedcakes, particularly derived from inedible seeds, have hazardous compounds that restrict their direct application [6]. It is therefore essential to further investigate their potential applications. De-oiled cakes can be transformed into valuable products and biofuels, which helps with their disposal problem and provides an additional means of addressing today's energy-related issues. Various thermochemical processes, including incineration, pyrolysis, and gasification have recently gained attention as effective methods for valorizing de-oiled seedcakes. The production of important products including pyro-gas, biochar, and bio-oil is made possible via pyrolysis [7]. The designing of a pyrolyzer requires consideration of the kinetic and thermodynamic characteristics. Thermogravimetric analysis (TGA) is a method to study the thermal degradation behavior of lignocellulosic biomasses.

Numerous studies have explored a wide range of biomass sources to assess their potential for biofuel production using various analytical techniques. For example, activation energy for the kinetic models of plum pomace was found to be 210 kJ/mol [8]. A kinetic analysis of garlic husk, using multiple isoconversional models, revealed an average activation energy between 153 and 155 kJ/mol [9]. Further studies focused on biomass from deciduous trees, specifically neem and gooseberry kernels, evaluated through TGA and model-free techniques. The activation energies for these materials were found to range from 176.66 to 204.23 kJ/mol for neem kernels and 184.57 to 195.10 kJ/mol for gooseberry kernels [10]. Other deciduous tree biomasses, such as date palm seed, and golden shower tree seeds, were also subjected to thermogravimetric and kinetic analyses, with activation energies ranging from 164 to 174 kJ/mol [11], [12]. Additionally, pyrolytic and kinetic studies on sawdust, using TGA and model-free methods, the study demonstrated that activation energies increased from 80 to 252 kJ/mol as the conversion process advanced[13]. Singh et.al [6] investigated the pyrolysis of mustard seedcake to

calculate activation energy of mustard oil residue (155 kJ/mol). Masawat et al. (2019)[14] used TGA to examine the pyrolysis properties of a Pongamia de-oiled cake and they found that the activation energy ranged from 97.2 to 412.2 kJ/mol. Sokoto et al. (2016) [15] examined the kinetics of seedcakes made from African star apples. They determined activation energy using the isoconversional approaches. Sahoo et al. [16] investigated the kinetics and thermodynamic parameters of a mixture of Pongamia pinnata and Sapindus emarginatus. Four model-free isoconversional techniques were used to derive the kinetic parameters. Hagig et.al [17] studied drying kinetics of hawthorn. A comprehensive review of existing literature highlights the significant potential of biomass from agricultural residues for pyrolytic and kinetic analysis, with many studies indicating the production of valuable pyrolysis products. However, it is evident that research focusing on the feasibility of converting biomass from neem trees into useful products remains limited.

Azadirachta indica, commonly known as neem, presents a reliable and sustainable feedstock option for biofuel production. Despite the widespread availability of neem, use of its seedcake as a feedstock for biofuel production remains underutilized. Neem seedcake can be thermally processed to produce biochar and biofuels, which have significant environmental benefits. NSC is rich in nitrogen and other nutrients, which adds value to the biochar produced from it. Biochar derived from NSC can serve as a soil conditioner, improving soil fertility and aiding in carbon sequestration. In the context of biofuels, these nanoparticle-enhanced fluids improve thermal properties, increasing the heat transfer efficiency of biofuel-based systems, which can enhance the overall energy performance of renewable energy processes [18]. Insulation-based systems can also be employed to enhance the efficiency of the existing system [19]. The study of its thermal degradation helps in developing biochar and biofuels with favorable properties for agronomic applications. Therefore, thermal degradation of NSC through pyrolysis presents a viable solution, enabling the breakdown of this abundant biomass into valuable biofuels and by-products.

The main objective of studying the thermal degradation behavior of NSC is to gain a comprehensive understanding of how this biomass decomposes under the influence of heat. This helps in modeling the decomposition behavior knowing the activation energy helps optimize the thermal processes used to convert biomass into useful products. The thermodynamic properties associated with the degradation process, provide insights into the energy requirements and efficiency of conversion processes. This knowledge is crucial for optimizing processes like pyrolysis, combustion, and gasification, which can convert neem seedcake into useful products such as biochar, bio-oil, and gases. The primary goal of this work was to evaluate kinetic parameters and thermodynamic properties of NSC pyrolysis.

In this study, three advanced isoconversional methods—Starink, Kissinger-Akahira-Sunose (KAS), and Ozawa-Flynn-Wall (OFW) are systematically applied to investigate the thermal degradation behavior of neem seedcake (NSC). Unlike model-fitting methods, isoconversional methods do not require a specific reaction model (such as first-order, second-order, etc.) to be assumed. This makes them more flexible and suitable for complex processes where the reaction mechanism is not fully understood or may change during the process [20]. These methods can be applied in diverse fields, such as polymer degradation, combustion, pyrolysis, oxidation reactions, and biomass conversion, where reactions may involve complex mechanism. These methods, which are widely recognized for their accuracy in evaluating the kinetics of thermal decomposition, have rarely been applied to NSC.

The novelty of this research is in its detailed examination of NSC's thermal and kinetic properties using isoconversional approaches to determine activation energy and reaction mechanisms without assuming a specific kinetic model. Moreover, current research on the pyrolysis of neem seedcake is scarce, particularly regarding its thermodynamic characteristics, kinetic parameters, and the thermal degradation patterns observed in the TGA and derivative thermogravimetric (DTG) analysis. This gap in knowledge makes the study particularly valuable, as it provides the comprehensive thermodynamic and kinetic analyses of NSC pyrolysis. The findings contribute to understanding of complex thermal reactions involved and lay groundwork for future research into optimizing biofuel production from NSC and similar non-edible oil seedcakes. By offering new data on reaction kinetics and degradation behavior, this study not only expands the scientific understanding of neem seedcake but also enhances its potential application in sustainable energy systems, positioning it as a promising feedstock for biofuel generation.

MATERIAL AND METHODS

Feedstock Characterization

The raw material used in this study was NSC, a byproduct of the oil extraction process, sourced from local oil mills. The ASTM D 3172-07 method was followed to determine moisture, ash, volatile matter, and fixed carbon of NSC. The de-oiled seedcakes were crushed and sieved to produce uniform size particles , dried in oven at 105 °C for 4 hours[21]. To assess the potential for converting NSC into value-added products, proximate analysis, ultimate analysis, and high heating value (HHV) were determined. The ultimate analysis identified the content of carbon (C), nitrogen (N), hydrogen (H), sulfur (S), and oxygen (O) in the NSC, using an Elementar Vario EL 111 model for C, H, N, S and O.

Thermogravimetric Study

The pyrolysis experiments were conducted using a cylindrical reactor made up of galvanized iron (GI), 80 mm of internal diameter and 75 mm of height was used to heat 100 grams of feedstock. The reactor used for pyrolysis was surrounded by a heater. A thermocouple was placed inside the reactor to monitor temperature of seed cake sample. A condenser was attached to reactor that condensed gases produced during pyrolysis. The bio-oil was taken in a flask at exit of condenser. A schematic illustrating setup used for these experiments is provided in Figure 1. J-type thermocouple, with an operating range of 0–750 °C and an accuracy of ±2.2%, was employed to record the pyrolysis temperature. The sample mass was measured using an Ohaus PR Precision Balance having a maximum capacity of 220 g. The overall uncertainty was determined using Holman's propagation of error approach, expressed through the square root method as given in Equation (1) [22–24]. Furthermore, Table 1 summarizes the accuracy, measurement range, and corresponding uncertainty values of the instruments used. Three sets of experiments were performed at 450°C, resulting in bio-oil, biochar, and pyrogas with an average value of 37.07%, 33.50% and 29.05% by weight respectively.

$$U_E = \left\{ \left[\left(\frac{\partial E}{\partial X_1} \right) u_1 \right]^2 + \left[\left(\frac{\partial E}{\partial X_2} \right) u_2 \right]^2 + \left[\left(\frac{\partial E}{\partial X_3} \right) u_3 \right]^2 + \cdots \left[\left(\frac{\partial E}{\partial X_n} \right) u_n \right]^2 \right\}^{1/2} \quad (1)$$

The total uncertainty associated with the measurement of weight (U_W, Eq. 2), temperature (U_T, Eq. 3), and total uncertainty (Eq. 4) was evaluated by considering instrument error, environmental effects, and calibration sensitivity. The combined uncertainty was then estimated using the root mean square (RMS) method.

$$U_W = \sqrt{I_W^2 + C_W^2 + R_W^2 + E_W^2} \quad (2)$$

$$U_T = \sqrt{I_T^2 + C_T^2 + R_W^2 + E_T^2} \quad (3)$$

$$total\ uncertainty = \sqrt{U_W^2 + U_T^2} \quad (4)$$

An SDT-Q600 thermal analyzer was used for TGA and DTG analysis. The 10 mg of NSC sample was carefully weighed and placed in a pan. The system was purged with an inert gas (nitrogen, 100 ml/min) to prevent unwanted reactions with atmospheric oxygen unless oxidative conditions are required. The furnace was then heated from ambient temperature to 800°C at desired heating rate (5°C/min, 10°C/min and 20°C/min). The TGA continuously recorded the sample's mass change with temperature. The uncertainty analysis for the instrument used is done as per as per Holman's square root rule[22], [23], [25] The range, resolution and sensitivity of the instrument is shown in Table 2.

The thermal decomposition behavior was analyzed using the Starink, KAS, and OFW methods. Applying

Table 1. Measurement range, accuracy, and associated uncertainty

Measuring Device	Range	Accuracy	Uncertainty (%)	Total uncertainty
Weighing scale	0-220 g	Uncertainty (I_W): ±0.001g	0.002	0.62%
		Calibration (C_W): ±0.001g		
		Environmental influence (E_W): ±0.001 g		
		Repeatability (R_W) : ±0.001g		
Thermocouple (J-type)	-200ºC-750ºC	Inherent uncertainty (I_T): ±2.2 ºC	0.62	
		Calibration (C_T): ±1ºC		
		Repeatability (R_T): ±1ºC		
		Environmental influence (E_T): ±1ºC		
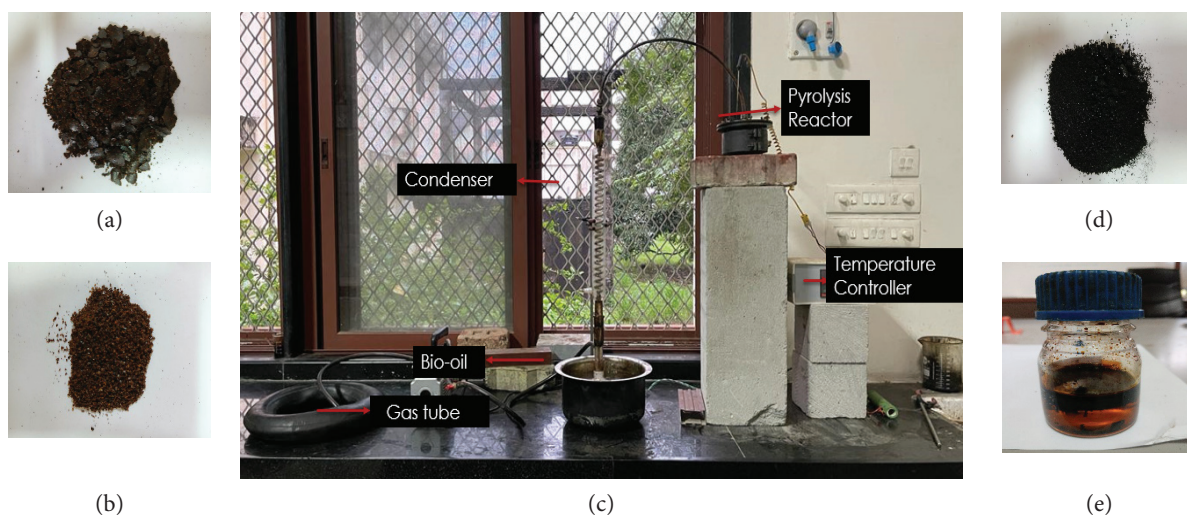
Figure 1. (a). Neem seedcake ;(b) Crushed seedcake; (c) lab-scale experimental setup; (d) biochar; (e) bio-oil.

Table 2. Parameters, range, resolution and uncertainty

Parameters	Range	resolution	Uncertainty (%)	Overall uncertainty
Measuring balance	0-200 mg	±0.1 µg	0.001	0.53%
DTG	ambient-1500ºC	±0.001ºC	0.000125	
Heating rate	0.1-25ºC/min	0.1ºC/min	0.5%	
Thermocouple	0-1500ºC	±1.5ºC	0.1875	

isoconversional kinetic models to analyze pyrolysis involves a step-by-step process to determine the activation energy and other thermodynamic parameters (Fig. 2).
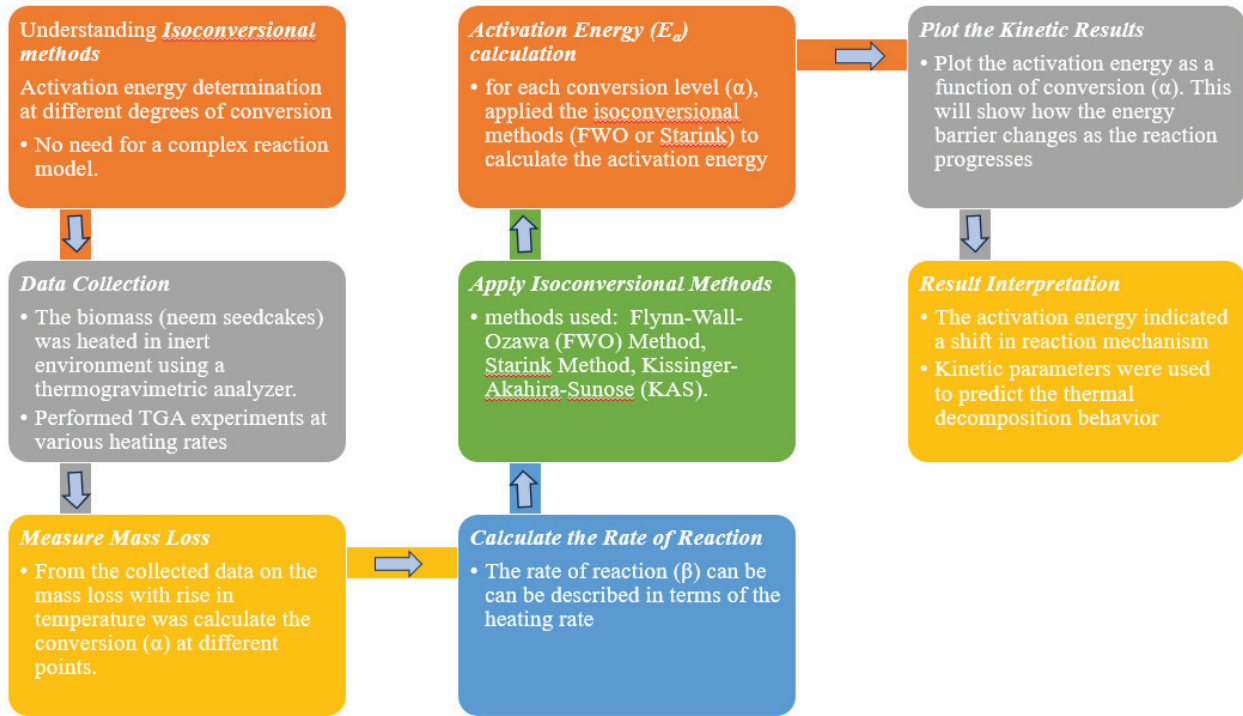
Kinetic Parameters

The thermal degradation of solid can be represented using following equations. The degree of conversion (α) was calculated using Equation (5).

$$\alpha = \frac{m_t - m_\infty}{m_0 - m_\infty} \qquad (5)$$

Here , initial sample mass is m_o, mass at time 't' is m_t, and final mass is m_∞. The decomposition rate is characterized by temperature function k(T) and conversion function f(α). The rate of reaction is determined by using equation (6).

$$\frac{d\alpha}{dt} = k(T) \times f(\alpha) \qquad (6)$$

The temperature function k(T) is expressed by equation (7).

Figure 2. A step-by-step process to determine kinetic and thermodynamic parameters.

$$k(T) = A exp(-E_\alpha/RT) \qquad (7)$$

Where, A, E_α, R and T are the pre-exponential factor, activation energy at α, gas constant and temperature respectively. The relationship between temperature (T) and time (t) is dT = βdt, where β is heating rate. So, Equation 6 is written as Equation (8).

$$\beta \frac{d\alpha}{dT} = A\, exp\left(\frac{-E_\alpha}{RT}\right) f(\alpha) \qquad (8)$$

Integrating the equation (8), is written as equation (9).

$$g(\alpha) = \oint \frac{d\alpha}{f(\alpha)} = \frac{A}{\beta} \oint exp\left(\frac{-E_\alpha}{RT}\right) dT = \frac{AE_\alpha}{\beta R}\, P(u) \qquad (9)$$

Where g(α) is the integral form of the reaction model and u = E_α/RT. P(u), is temperature integral. The objective of the kinetic analysis is to develop mathematical correlations between temperature, conversion extent, and process rate. The parameter Eα denotes the activation energy barrier, while A reflects the frequency factor related to the vibrations of the activated complex. The reaction pathway is interpreted using either f(α) or g(α) [26],[27]. In the study of reaction kinetics, particularly for complex reactions, the lack of an explicit solution for the temperature-dependent function P(u) necessitates the use of approximation methods. Acar et.al [28] explored various drying models to identify the most suitable one for predicting moisture loss and drying kinetics. Without assuming a reaction mechanism,

E_α can be estimated using isoconversional methods [16]. The ICTAC Kinetics Committee suggests commonly applied integral isoconversional approaches, namely Starink, KAS, and OFW [17]. These techniques allow the determination of kinetic parameters without requiring an explicit expression for P(u).

Thermodynamic Properties

The thermodynamic properties, specifically the enthalpy change (ΔH), the Gibbs free energy change (ΔG), and the entropy change (ΔS) were determined using the E_α and A values calculated from Starink, KAS, and OFW methods using following equations (10), (11), (12) and (13).

$$A = \frac{\beta E_\alpha exp(\frac{E_\alpha}{RT_m})}{RT_m^2} \qquad (10)$$

$$\Delta H = E_\alpha - RT \qquad (11)$$

$$\Delta G = E_\alpha + RT ln(\frac{K_B T_m}{hA}) \qquad (12)$$

$$\Delta S = (\Delta H - \Delta G)/T_m \qquad (13)$$

where K_B is the Boltzmann constant (1.381×10^{-23} J/K), h is the Plank constant (6.626×10^{-34} J.s), and T_m is DTG (derivative thermogravimetric) peak temperature (K).

RESULTS AND DISCUSSIONS

Characterization of NSC

The proximate and ultimate analyses, along with the higher heating value (HHV) of NSC (Table 3), were conducted to assess their suitability for the pyrolysis process and compare their characteristics with those of other biomass materials. The volatile matter (VM) content should be between 70-80%, with ash content below 10%. These characteristics high VM and low ash content indicate suitability of such feedstocks for thermal processes. The ultimate analysis revealed that NSC has carbon content (≥43%), making it viable option for fuel and energy recovery. Additionally, the low sulfur and nitrogen content in NSC suggests that the generation of SOx and NOx during pyrolysis would be minimal. The HHV of feedstock is 20.40 MJ/kg, comparable to HHVs of similar biomasses used in pyrolysis, like peanut shells and de-oiled mustard cake (19.4 MJ/kg)[6], (18.95 MJ/kg)[29], beauty leaf seedcake (19.20 MJ/kg)[30] and macadamia nutshell (19.367 MJ/kg)[31]. Overall, the proximate composition of NSC lies within the typical range reported for other biomass feedstocks utilized in pyrolysis. The HHV was measured by using equation (14)[32].

$$HHV \left(\frac{MJ}{kg}\right) = 0.3491C + 1.1783\,H - 0.1034\,O + 0.1005\,S - 0.0151\,N \tag{14}$$

Thermogravimetric Analysis

The TGA profile of NSC under a nitrogen atmosphere (0.1 L/min) at three different heating rates is presented in Fig. 3(a). The analysis indicates that temperature range of 220–550 °C representing active pyrolysis zone. Three distinct weight-loss phases are observed in the TGA curve. In the initial stage, from ambient temperature up to 220 °C, the decomposition is minimal, primarily involving moisture removal (~8%). The second stage, occurring between 220 °C and 550 °C, exhibits a pronounced weight loss (~74%), as reflected by a sharp decline in the TGA curve and a prominent peak in the DTG plot [33]. During this phase, feedstock undergoes cracking reactions, and decarboxylation, leading to the evolution of volatiles and char formation [34]. This stage represents the active pyrolytic zone, where the majority of decomposition occurs and the char residue is formed. The third stage, observed at temperatures above 550 °C, corresponds to the passive pyrolysis zone. Here, residual chemical bonds are broken, and the remaining molecular skeletons undergo slow degradation [35]. Lignin decomposition dominates this stage, while cellulose degradation contributes to the central DTG peak observed between 320–370 °C [16],[37]. Comparatively, other de-oiled biomass feedstocks show DTG peaks in similar ranges, such as mustard oil residue (170–510 °C) [6] and African star apple (150–400 °C) [36].

Table 3. Ultimate analysis, proximate analysis, and HHV of neem seedcake

NSC	Proximate analysis				Ultimate Analysis					HHV (MJ/kg)
	Volatile matter (%)	Moisture (%)	Fixed Carbon (%)	Ash (%)	C (%)	N (%)	O (%)	S (%)	H (%)	
	77.83	7.13	6.91	8.13	48.88	3.00	42	0.00	6.48	20.40
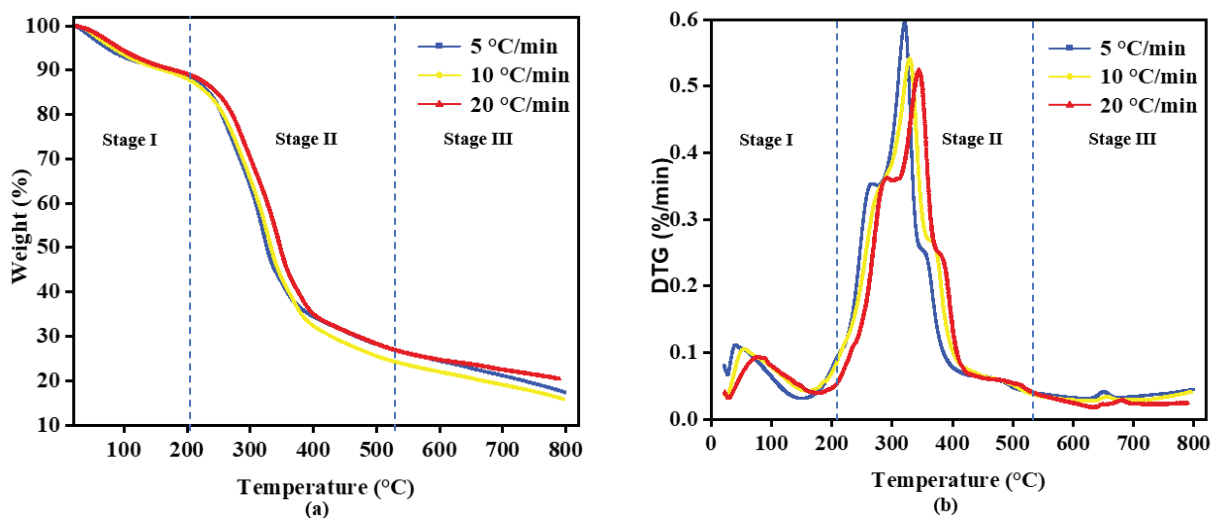
Figure 3. (a) Thermogravimetric Analysis (TGA) and (b) Derivative Thermogravimetric (DTG) curves for neem seedcake pyrolysis at varying heating rates.

The peak temperatures recorded for NSC during thermal degradation were 323, 330, and 340 °C at heating rates of 5, 10, and 20 °C/min, respectively, with corresponding residual masses of 17.32%, 15.89%, and 20.39%. These peak values were determined from the DTG curves (Fig. 3(b)), highlighting dependence of thermal decomposition on the heating rate.

Kinetic Parameters

Three model-free isoconversional approaches: Starink, KAS, and OFW methods were used to determine the kinetic parameters [38]. The isoconversional principle asserts that temperature alone determines the reaction rate at a given degree of conversion. This can be demonstrated by evaluating logarithmic derivative of equation (6), at α = const.

$$\left[\left(\frac{\partial ln\left(\frac{d\alpha}{dt}\right)}{\partial T^{-1}}\right)\right]_\alpha = \left[\left(\frac{\partial lnk(T)}{\partial T^{-1}}\right)\right]_\alpha + \left[\left(\frac{\partial lnf(\alpha)}{\partial T^{-1}}\right)\right]_\alpha \quad (15)$$

The subscript denotes values corresponding to a particular degree of conversion, representing isoconversional data. The second term in eq. (15) is zero, and f(α) remains constant when α=const.

$$\left[\left(\frac{\partial ln\left(\frac{d\alpha}{dt}\right)}{\partial T^{-1}}\right)\right]_\alpha = -\frac{E_\alpha}{R} \quad (16)$$

The relation in the equation above is used to determine the E_α of biomass using model-free method, without any reaction model assumption. The factor A, E_α, and coefficient of determination (R^2) were determined at fixed conversions, for temperature range from ambient to 800°C [33]. It is suggested to determine E_α within α = 0.05 to 0.95 with a step size not larger than 0.05 [38]. During the first stage, E_α increases slowly up to a 0.20 conversion, indicating low reactivity up to 220°C, where only moisture and impurities were removed. During the second stage, from 0.20 to 0.75 conversion, E_α increased as the devolatilization process occurred, decomposing the volatile matter present in NSC between 220 and 550°C. Beyond a 0.75 conversion, activation energy decreased due to minimal amount of volatile matter remaining. The isoconversional models by Starink, KAS, and OFW are expressed as equation (17), equation (18), and equation (19).

$$\ln\left(\frac{\beta}{T^{1.92}}\right) = Constant - 1.0008\frac{E_\alpha}{RT} \quad (17)$$

Therefore, a plot of ln(β/T^1.92) vs 1/T, will be a straight line for given α. The E_α is calculated using slope of straight line, or −1.008 E_α/R.

$$\ln\left(\frac{\beta}{T^2}\right) = Constant - \frac{E_\alpha}{RT} \quad (18)$$

Therefore, a plot of ln(β/T²) versus 1/T, at various heating rates, will be a straight line for given α. The E_α is calculated using slope of straight line, or −E_α/R.

$$\ln(\beta) = Constant - 1.052\frac{E_\alpha}{RT} \quad (19)$$

Therefore, a plot of ln(β) versus 1/T, at various heating rates will be a straight line for given α. E_α is calculated as −1.052 E_α/R, slope of straight line.

Linear plots for Starink, KAS, and OFW methods are presented in Fig. 4(a), 4(b), and 4(c), respectively. These plots are employed to evaluate E_α across a conversion range of α=0.05–0.95. For neem seedcake, this plot helps to identify how the activation energy changes as the pyrolysis progresses. This method is particularly useful in determining the multi-step nature of biomass pyrolysis reactions, as deviations from linearity can indicate changes in reaction mechanisms. During the pyrolysis of NSC, the activation energy may vary across different stages, reflecting multiple reaction mechanisms. The variation in activation energy indicates the involvement of numerous overlapping reactions with distinct energy barriers, particularly the decomposition of hemicellulose and lignin. The reliability of the selected kinetic methods is indicated by R^2>0.90. The activation energy (E_α) increases with conversion (α) due to the occurrence of multiple endothermic reactions and sequential decomposition of cellulose, lipids, and proteins at different temperatures [26]. As shown in Table 4, the activation energy (E_α) varies with conversion, ranging from 73.14 to 429.28 kJ/mol, 72.9664-429.336 kJ/mol, and 69.3534–415.2271 kJ/mol, for Starink, KAS, and OFW approaches with the value ($R^2 \geq 0.90$), respectively. The average values of E_α obtained by the Starink, KAS, and OFW methods are 249.258 kJ/mol, 230.853 kJ/mol, and 228.026 kJ/mol. The variation of E_α with alpha is shown in Fig. 5.

Equation (10) was used to calculate factor A. The number of molecular collisions required for a reaction is measured by A. For A <10^9 s^{-1}, the reaction is surface-dependent, and A >10^9 s^{-1} suggests a complex reaction[26]. For NSC, values of A ranged from 10^{14} to 10^{37} at 0.05 to 0.95 conversions, indicating the presence of complex reactions. Table 4 presents value of 'A' evaluated using Starink, KAS, and OFW methods, ranging from 10^{12}- 10^{35}, 10^{12}–10^{35}, and 10^{12}–10^{34} s^{-1}, respectively. Table 4 indicates the variation of factor 'A' with conversion similar to the changes in E_α, and the wide range of 'A' suggests that NSC decomposition is complex. At a 0.20 conversion, both E_α and A were quite low, while at a 0.75 conversion, they were A = 10^{35}-10^{37} s^{-1} and E_α = 415.22-429.28 kJ/mol, indicating low reactivity at 0.20 conversion and the highest reactivity at 0.75 conversion. The average value of 'A' was 9.16×10^{33}, 9.3×10^{33}, and 1.7×10^{33}s−1 for Starink, KAS, and OFW methods, respectively.
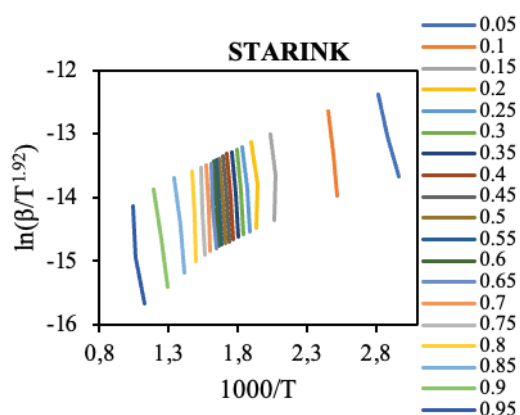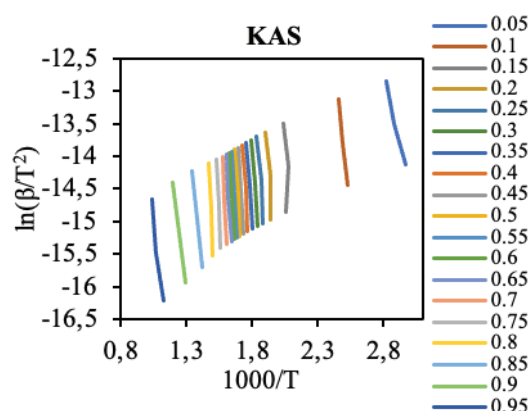
Figure 4. (a) ln(β/T1.92) vs (1/T) for Starink.

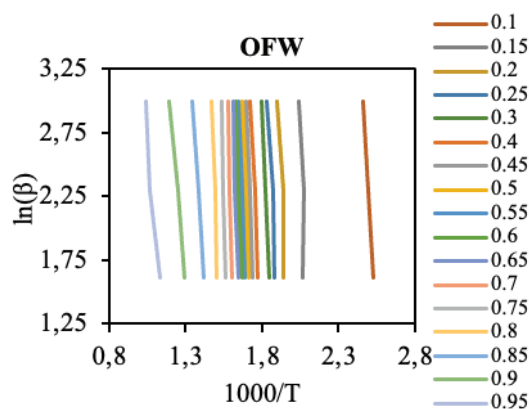**Figure 4.** (b) ln(β/T2) vs (1/T) plot for Kissinger-Akahi-ra-Sunose.

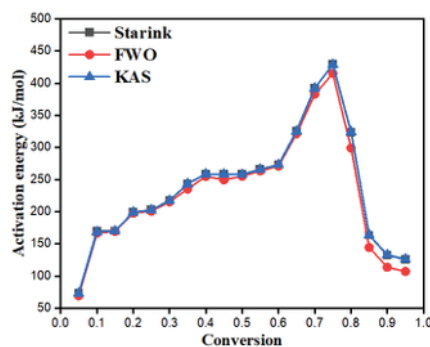**Figure 4.** (c) ln(β) vs (1/T) plots for Ozawa-flynn-wall.

Figure 5. The variation in activation energy to conversion rate for neem seedcake.

Thermodynamic Analysis

Understanding the energy potential and distribution of a reaction requires understanding its thermodynamic properties ΔH, ΔG, and ΔS. ΔH_α, ΔG_α, and ΔS_α were determined for NSC at 20°C/min (Table 5). These properties were determined by substituting E_α values into Equations (11), (12), and (13) respectively. The graph of enthalpy change (ΔH) versus conversion rate (α) (Fig. 6) for the decomposition of neem seedcake provides insights into the energy requirements and reaction characteristics at different stages of thermal degradation process. In the initial phase, evaporation of moisture and release of some volatiles take place, which are relatively low-energy processes. At this stage, the neem seedcake is only undergoing minor thermal decomposition, so energy demand is minimal. The positive values of ΔH indicate that reaction is primarily endothermic. In the second phase, the endothermic nature of the process becomes prominent as the structural components of neem seedcake undergo degradation. The breakdown of hemicellulose and cellulose,

which requires significant energy to break the polymeric bonds, results in a high positive enthalpy change. This rise in enthalpy change shows the energy absorbed by the system to facilitate these reactions. In the final stage ($\alpha > 0.75$), as the conversion progresses and the remaining biomass becomes more carbonized (biochar formation), the energy requirement for decomposition decreases and some exothermic reactions take place, which results in slight decrease in enthalpy change. The average values of ΔH for NSC are 244.162 kJ/mol, 235.918 kJ/mol, and 222.961 kJ/mol using Starink, KAS, and OFW methods, respectively.

The Gibbs free energy (ΔG) versus the conversion rate (α) graph (Fig. 7) represents the thermodynamic favorability of the process at different stages of the decomposition. Gibbs free energy, the energy available for utilization after the reaction, was also calculated. At initial phase of decomposition ΔG is maximum. This indicates that the reaction is less thermodynamically favorable, as reactant is in the stable form, requiring

an input of energy to initiate breakdown. In the middle phase (0.2<α<0.75), is a negative slope region, indicates the decomposition is thermodynamically favorable as ΔG decreases with increasing conversion rate. Toward the end of the reaction, as α approaches 1, the graph may show a slight rise in ΔG. The system approaches equilibrium, with the diminishing driving force for the reaction. The average values of ΔG are 172.973, 172.966, and 167.582 kJ/mol for Starink, KAS, and OFW methods, respectively. From Fig. 5 and Fig. 6, it is evident that both E_α and ΔH_α increase from 0.20 to 0.75 conversion, indicating a rise in endothermicity, and after that, the exothermic reactions become pronounced. The ΔG in the present study were compared to those found in other studies, such as bamboo (101.28–113.95 kJ/mol) [39] and sewage sludge (71.78–92.94 kJ/mol)[33].

ΔS, with a positive value indicating more disorder in the products. Fig. 8 represents the graph of entropy change (ΔS) versus conversion rate (α). In the initial phase of decomposition (α< 0.2), entropy change is usually low or negative. Negative entropy change indicates that the system becomes more ordered, which might be attributed to the release of low-energy volatiles or residual water, reducing the overall complexity of the remaining solid structure. As the conversion increases, the change in entropy begins to increase. This is the phase where major structural breakdown of the neem seedcake

occurs, with hemicellulose and cellulose undergoing thermal decomposition. At high conversion rates (α > 0.75), the change in entropy decreases slightly. This stage represents the final breakdown of the lignin structure and the formation of more stable biochar. The average ΔS values were 0.09453, 0.09443, and 0.09034 for Starink, KAS and OFW methods, respectively. Table 5 shows the ΔH_α, ΔG_α, and ΔS_α values for conversions from 0.05 to 0.95. The changes in the thermodynamic characteristics of the NSC pyrolysis imply a complicated reaction chemistry. During pyrolysis, the entropy (ΔS) of the system changes as the solid NSC material breaks down into smaller molecules (gases and liquids), increasing disorder in the system. These pathways are often complex, with a variety of chemical bonds breaking and forming, contributing to a broad distribution of products. This reflects the diversity of reactions taking place, such as the cracking of long-chain hydrocarbons or the formation of aromatic compounds. Pyrolysis typically involves endothermic steps where heat is absorbed (e.g., breaking of chemical bonds in cellulose and lignin) and exothermic steps where heat is released (e.g., the formation of biochar and the release of volatile compounds). The presence of both endothermic and exothermic reactions in different stages of NSC pyrolysis highlights the simultaneous occurrence of competing reactions.

Table 4. Activation energy, pre-exponential factor and coefficient of determination

	KAS			OFW			STARINK		
α	E_α (kJ/mol)	A(s^{-1})	R^2	E_α (kJ/mol)	A (s^{-1})	R^2	E_α (kJ/mol)	A (s^{-1})	R^2
0.05	72.96639	771295.5	0.9939	69.35336	360813.7	0.9939	73.13736	799477.708	0.993
0.01	168.5515	2.49E+14	0.9998	166.5666	1.67E+14	0.9998	170.1199	3.4178E+14	0.9998
0.15	169.9318	3.29E+14	0.3627	169.2222	2.85E+14	0.3845	170.1199	3.4178E+14	0.3636
0.20	199.3152	1.23E+17	0.7097	197.7065	8.91E+16	0.7269	199.5048	1.2793E+17	0.7104
0.25	202.641	2.4E+17	0.9182	200.9153	1.7E+17	0.9245	202.6119	2.3903E+17	0.9185
0.30	217.4075	4.68E+18	0.9678	215.355	3.1E+18	0.9703	217.5993	4.8594E+18	0.9679
0.35	243.3488	8.5E+20	0.9829	235.4221	1.74E+20	0.988	243.5281	8.8103E+20	0.983
0.40	258.6392	1.81E+22	0.9841	254.9042	8.59E+21	0.9852	258.8146	1.8796E+22	0.9841
0.45	258.2899	1.69E+22	0.9844	249.6958	3.03E+21	0.988	258.4739	1.7557E+22	0.9845
0.50	257.9407	1.58E+22	0.9915	255.0939	8.93E+21	0.9856	258.1499	1.6455E+22	0.9915
0.55	265.8645	7.7E+22	0.9995	263.5823	4.88E+22	0.9996	266.1089	8.0855E+22	0.9995
0.60	273.0482	3.24E+23	0.9982	271.0037	2.15E+23	0.9979	273.3118	3.4127E+23	0.9982
0.65	325.3131	1.1E+28	0.9703	321.5388	5.17E+27	0.9996	325.5682	1.1537E+28	0.9703
0.70	392.4436	6.95E+33	0.9835	382.791	1.02E+33	0.9843	392.5378	7.0813E+33	0.9835
0.75	429.3358	1.06E+37	0.9917	415.2271	6.43E+35	0.9913	429.2834	1.0477E+37	0.9916
0.80	324.2572	8.88E+27	0.9693	299.0691	5.85E+25	0.9295	323.5909	7.7795E+27	0.9251
0.85	164.0035	9.92E+13	0.9978	144.4921	1.9E+12	0.9981	163.3906	8.7656E+13	0.9978
0.90	133.19	1.91E+11	0.9984	113.5182	3.43E+09	0.9478	132.5352	1.6694E+11	0.9369
0.95	125.9564	4.36E+10	0.9105	107.0294	9.04E+08	0.9986	125.324	3.835E+10	0.9982

Table 5. Thermodynamic parameters (ΔHα, ΔGα, and ΔSα) for NSC

	KAS			OFW			STARINK		
α	ΔH (kJ/mol)	ΔG (kJ/mol)	ΔS (kJ/mol.K)	ΔH (kJ/mol)	ΔG (kJ/mol)	ΔS (kJ/mol.K)	ΔH (kJ/mol)	ΔG (kJ/mol)	ΔS (kJ/mol.K)
0.05	70.01964	178.5472	-0.17704	66.40661	173.2069	-0.17423	70.19061	178.538	-0.17675
0.01	165.1701	174.2802	-0.01486	163.1852	168.7415	-0.00906	166.7385	174.2394	-0.01224
0.15	165.85	174.2386	-0.01368	165.1405	168.6609	-0.00574	166.0382	174.2394	-0.01338
0.20	194.9368	173.4258	0.035091	193.3281	167.868	0.041534	195.1264	173.4284	0.035396
0.25	198.108	173.3414	0.040402	196.3823	167.7859	0.04665	198.079	173.3498	0.040341
0.30	212.7732	172.9829	0.064911	210.7206	167.4322	0.070617	212.9649	172.9867	0.065217
0.35	238.623	172.4085	0.108017	230.6963	166.9782	0.103945	238.8023	172.4139	0.108301
0.40	253.8206	172.0979	0.133316	250.0857	166.573	0.136236	253.9961	172.1042	0.133592
0.45	253.3812	172.1048	0.132588	244.7871	166.6782	0.127421	253.5652	172.1109	0.132878
0.50	252.9551	172.1117	0.131882	250.1083	166.5692	0.136279	253.1644	172.1173	0.132214
0.55	260.8174	171.9575	0.144959	258.5352	166.4023	0.150298	261.0618	171.9628	0.145349
0.60	267.944	171.8216	0.156807	265.8995	166.2608	0.162543	268.2076	171.827	0.157228
0.65	320.1522	170.929	0.243431	316.3779	165.3894	0.246311	320.4073	170.9373	0.243834
0.70	387.1688	169.9729	0.354316	377.5162	164.5007	0.347497	387.263	169.9865	0.354448
0.75	423.9138	169.515	0.415006	409.805	164.0862	0.400846	423.8613	169.5318	0.414893
0.80	318.5938	170.9456	0.240862	293.4057	165.7586	0.208233	317.9275	170.9683	0.239738
0.85	157.8094	174.4196	-0.0271	138.298	169.466	-0.05085	157.1965	174.4448	-0.02814
0.90	126.2216	175.4802	-0.08036	106.5499	170.6956	-0.10464	125.5669	175.5103	-0.08147
0.95	117.9565	175.7648	-0.0943	99.02961	170.9956	-0.1174	117.3242	175.7952	-0.09539
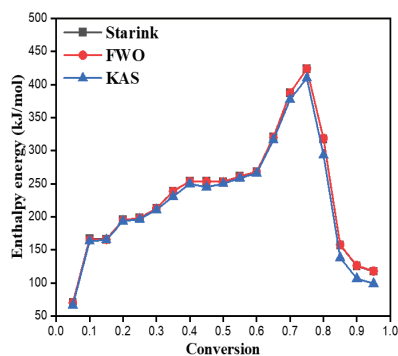
Figure 6. ΔH to alpha(α) for neem seedcake.
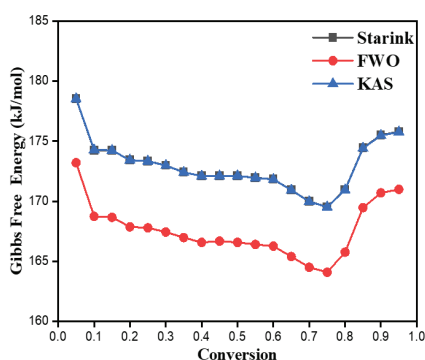
Figure 7. ΔG to alpha(α) for neem seedcake.
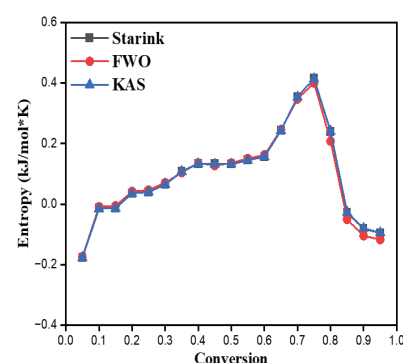
Figure 8. ΔS to alpha(α) for neem seedcake.

CONCLUSIONS

This study investigated thermal decomposition behavior, kinetics, and thermodynamic properties of NSC through TGA experiments. Three model-free methods (Starink, KAS, and OFW) were used to estimate pyrolysis activation energy of NSC. Based on experimental investigation, following conclusions can be summarized:

- The data showed that NSC decomposition proceeded in three stages, with the active pyrolysis taking place between 220 and 550 °C.

- The activation energies for NSC pyrolysis, computed using the Starink, Kissinger-Akahira-Sunose (KAS), and Ozawa-Flynn-Wall (OFW) methods were 235.985 kJ/mol, 235.918 kJ/mol, and 228.026 kJ/mol, respectively.

- The thermodynamic analysis indicated complex reaction chemistry in the NSC sample, involving both volatile organic compounds. Thermodynamic parameters indicated that endothermic behavior increased, as α increased from 0.20 to 0.75, with the product having the highest activation energy at α = 0.75.

The study of thermodynamic properties and thermal degradation behavior of NSC has several practical applications, especially in the fields of bioenergy, and environmental sustainability. These findings are significant for predicting reaction performance and optimizing energy pyrolysis processes. These studies help optimize biomass conversion technologies, develop new materials, and assess the environmental impact of thermal processes. It contributes to the efficient utilization of neem seedcake, an agricultural byproduct, by converting it into valuable products through thermochemical processes.

The study of the thermal degradation behavior of biomass faces several limitations, which can affect the accuracy and generalizability. Biomass can vary significantly in composition depending on its type (e.g., wood, agricultural residues, algae), moisture content, and geographical origin. The rate at which biomass is heated influences the decomposition process. Slow heating might result in different degradation pathways compared to rapid heating, making it challenging for large-scale applications where heating rates can vary. These variations lead to inconsistent degradation behavior. The pyrolysis process for industrial applications requires further investigation into how the kinetic and thermodynamic parameters of neem seedcake change in larger reactors.

Future Recommendations

The model-free methods provide reliable activation energy data, future studies could focus on refining kinetic models by integrating machine learning to predict the behavior of complex biomass like neem seedcake. While significant progress has been made in understanding the pyrolysis mechanism of neem seed cakes (NSC), several aspects remain unclear, particularly regarding the intricate details of the decomposition pathways and the formation of intermediate compounds. Kinetic models that account for the formation and decomposition of intermediate species could provide more clarity on the specific pathways involved. The effect of varying temperatures and residence times on the rate of decomposition and the distribution of products remains unclear. The effect of varying temperatures and residence times on the rate of decomposition and the distribution of products remains unclear. Developing temperature-dependent kinetic models could help to better characterize these dynamics.

Advanced spectroscopic or imaging methods can be incorporated that could provide more detailed insights into the thermal breakdown mechanisms, chemical transformations, and structural changes occurring during pyrolysis. These advanced experimental techniques (FTIR, Raman, GC-MS), morphological changes (SEM, XRD), and elemental transformations (XPS, EDS)) will offer a more detailed characterization of both the solid (biochar) and volatile (gaseous and liquid) products formed during the pyrolysis of NSC. These techniques will collectively offer a more comprehensive understanding of NSC components (cellulose, hemicellulose, lignin, proteins) decomposition and contribute to biochar formation and gas evolution.

AUTHORSHIP CONTRIBUTIONS

Authors equally contributed to this work.

DATA AVAILABILITY STATEMENT

The authors confirm that the data that supports the findings of this study are available within the article. Raw data that support the finding of this study are available from the corresponding author, upon reasonable request.

CONFLICT OF INTEREST

The author declared no potential conflicts of interest with respect to the research, authorship, and/or publication of this article.

ETHICS

There are no ethical issues with the publication of this manuscript.

STATEMENT ON THE USE OF ARTIFICIAL INTELLIGENCE

Artificial intelligence was not used in the preparation of the article.

NOMENCLATURE

Symbol	Description
α	Degree of conversion
t	Time, s
T	Absolute temperature, K
β	Heating rate (dT/dt), K/s
$k(T)$	Rate constant at temperature T, 1/s
A	Pre-exponential factor (Arrhenius parameter), 1/s
E_α	Activation energy, kJ/mol
R	Universal gas constant (8.314 J/mol·K), J/mol.K
$f(\alpha)$	Reaction model function (depends on the reaction mechanism)
$g(\alpha)$	Integral form of reaction model
$\ln$	Natural logarithm
ΔT	Temperature interval, K
$T_\alpha(\alpha)$	Temperature corresponding to a specific α, K
$E_\alpha(\alpha)$	Activation energy as a function of conversion, kJ/mol

REFERENCES

[1]　Nguyen VG, Dager B, Chhilar A, Sharma P, MO Sameh, DTN Le, et al. Desirability-based optimization of dual-fuel diesel engine using acetylene as an alternative fuel. Case Stud Therm Eng 2024;59: 104488. [Crossref]

[2]   Kassim FO, Thomas CLP, Afolabi OOD. Integrated conversion technologies for sustainable agri-food waste valorization: A critical review Biomass Bioenergy 2021;156:106314. [Crossref]

[3]   Khandelwal N, Yadav P, Said Z, Sharma M, Shukla AK, Singh O, et al. A Comprehensive analysis of energy, exergy, economic and environment on integrated solarcombined cycle with various HTFs and thermal storage. Appl Energy 2024;37:6124203. [Crossref]

[4]   Agrawalla A, Kumar S, Singh RK. Pyrolysis of groundnut de-oiled cake and characterization of the liquid product. Bioresour Technol 2011;102:10711–10716. [Crossref]

[5]   Yadav PS, Said Z, Gautam R, Raman R, Caliskan H. Novel investigation on atomization, performance, and emission characteristics of preheated jatropha oil methyl ester and ethyl ester. Energy 2022;270;126870. [Crossref]

[6]   Kumar Singh R, Patil T, Pandey D, Sawarkar AN. Pyrolysis of mustard oil residue: A kinetic and thermodynamic study. Bioresour. Technol 2021;339;125631. [Crossref]

[7]   Silvestre WP, Pauletti GF, Baldasso C. Fodder radish (Raphanus sativus L.) seed cake as a feedstock for pyrolysis. Ind Crops Prod 2020;154:112689. [Crossref]

[8]   Đ. Katnić, Marinović-Cincović M, Katnić*et* SP, Vujčić IT. Characterization and kinetics of thermal decomposition behavior of plum and fig pomace biomass. J Clean Prod 2022;352:131637. [Crossref]

[9]   Singh RK, Pandey D, Patil T, Sawarkar AN. Pyrolysis of banana leaves biomass: Physico-chemical characterization, thermal decomposition behavior, kinetic and thermodynamic analyses. Bioresour Technol 2020;310:123464. [Crossref]

[10]   Mishra RK, Mohanty K. Kinetic analysis and pyrolysis behaviour of waste biomass towards its bioenergy potential. Bioresour Technol. 2020;311:123480. [Crossref]

[11]   Sahoo A, Kumar S, Mohanty K. Kinetic and thermodynamic analysis of Putranjiva roxburghii (putranjiva) and Cassia fistula (amaltas) non-edible oilseeds using thermogravimetric analyzer. Renew Energy 2021;165:261–277. [Crossref]

[12]   Pal DB. Thermo-chemical potential of solid waste seed biomass obtained from plant Phoenix dactylifera and Aegle marmelos L. Fruit core cell. Bioresour Technol 2021;345:126441. [Crossref]

[13]   Kristanto J, Daniyal AF, Pratama DY, Noer I. Kinetic Study on The Slow Pyrolysis of Isolated Cellulose and Lignin from Teak Sawdust. Thermochim Acta 2022;711:179202. [Crossref]

[14]   Masawat N, Atong D, Sricharoenchaikul V. Thermo-kinetics and product analysis of the catalytic pyrolysis of Pongamia residual cake. J Environ Manage 2019;242:238–245. [Crossref]

[15]   Sokoto MA, Singh R, Krishna BB, Kumar J, Bhaskar T. Non-isothermal kinetic study of de-oiled seeds cake of African star apple (Chrosophyllum albidum) using thermogravimetry. Heliyon 2016:10;2. [Crossref]

[16]   Sahoo A, Gautam R, Kumar S, Mohanty K. Energy optimization from a binary mixture of non-edible oilseeds pyrolysis: Kinetic triplets analysis using Thermogravimetric Analyser and prediction modeling by Artificial Neural Network. J Environ Manage 2021;297:113253. [Crossref]

[17]   Hagig KA, Acar B, Dağdeviren A, Taşkesen E, Özkaymak M. Freeze-drying kinetics and diffusion modeling of hawthorn. J Therm Eng 2023;9:876–884. [Crossref]

[18]   Dağdeviren A, Gedik E, Keçebaş A, Pazarlıoğlu HK, Arslan K, Alsabery AI. Effect of Al 2 O 3 – SiO 2 /Water Hybrid Nanofluid Filled in a Square Enclosure on the Natural Convective Heat Transfer Characteristics: A Numerical Study. J Nanofluids 2022;11:772–781. [Crossref]

[19]   Dagdeviren A, Acar B, Aydın M.Alternative heat insulation method for rigid construction walls. Int J of Energy Stud 2021;6:19–35.

[20]   Ponnam V, Ghodke P, Tondepu S, Mandapati RN. Thermal Behaviour Kinetic Modeling of Capsicum Annuum Waste Biomass Using an Iso-Conversion Method. J Therm Eng 2021;7:18–29. [Crossref]

[21]   Bhattacharjee N, Biswas AB. Pyrolysis of orange bagasse: Comparative study and parametric influence on the product yield and their characterization. J Environ Chem Eng 2019;7:102903.[Crossref]

[22]   Yadav PS, Ahmed SFA, Gautam R, Caliskan H, Caliskan N, Hong H. Nozzle effects on spray combustion and emissions in compression ignition engines using waste cooking oil biodiesel: A computational fluid dynamics analysis at varying injection pressures. IET Renew Power Gener 2023;2340–2359. [Crossref]

[23]   Yadav PS, Gautam R. Numerical and experimental analysis on spray characteristics of biodiesel (waste cooking oil) using pressure swirl atomizer. Environ Prog Sustain Energy 2021. [Crossref]

[24]   Patel PM, Rathod VP, Patel VK. Development and enhancement in drying performance of a novel portable greenhouse solar dryer. J Stored Prod Res 2024;105:102228. [Crossref]

[25]   Yadav PS, Gautam R, Le TT, Khandelwal N, Le AT, Hoang AT. A comprehensive analysis of energy, exergy, performance, and emissions of a spark-ignition engine running on blends of gasoline, ethanol, and isoamyl alcohol. Energy 2024;307:132548. [Crossref]

[26]   Mphahlele K, Matjie RH, Osifo PO. Thermodynamics, kinetics and thermal decomposition characteristics of sewage sludge during slow pyrolysis. J Environ Manage 2021;284:112006. [Crossref]

[27] Tagade A, Kandpal S, Sawarkar AN. Insights into pyrolysis of pearl millet (Pennisetum glaucum) straw through thermogravimetric analysis: Physico-chemical characterization, kinetics, and reaction mechanism. Bioresour Technol 2024;391:129930. [Crossref]

[28] Acar B, Dağdeviren A Ozkaymak M. Design of hazelnut drying system supported by solar energy, investigation of drying performance and determination of proper drying model. Int J Renew Energy Res 2020;10: 570–577.

[29] Kumar M, Rai D, Bhardwaj G, Upadhyay SN, Mishra PK. Pyrolysis of peanut shell: Kinetic analysis and optimization of thermal degradation process. Ind Crops Prod 2021;174:114128. [Crossref]

[30] Ashwath N, Nam H, Capareda S. Maximizing energy recovery from beauty leaf tree (Calophyllum inophyllum l.) oil seed press cake via pyrolysis. Energies 2021;9:14. [Crossref]

[31] Hasan MM, Rasul MG, Jahirul MI, Khan MMK. Fast pyrolysis of macadamia nutshell in an auger reactor : Process optimization using response surface methodology (RSM) and oil characterization. Fuel 2023;333:126490. [Crossref]

[32] Dhanavath KN. Optimization of process parameters for slow pyrolysis of neem press seed cake for liquid and char production. J Environ Chem Eng 2019;7:102905. [Crossref]

[33] Soni NK, Prabhansu, Bhale PV. Chemical insight into thermal degradation, chemical kinetics, and thermodynamics behavior of sewage sludge through thermogravimetry and Fourier transform infrared analysis. Therm Sci Eng Prog 2024;51:102617. [Crossref]

[34] Ordonez-Loza J, Chejne F, Jameel AGA, Telalovic S, Arrieta AA, Sarathy SM. An investigation into the pyrolysis and oxidation of bio-oil from sugarcane bagasse: Kinetics and evolved gases using TGA-FTIR. J Environ Chem Eng 2021;9:5. [Crossref]

[35] Volli V, Singh RK. Production of bio-oil from de-oiled cakes by thermal pyrolysis. Fuel 201;96:579–585. [Crossref]

[36] Sokoto MA, Biswas B, Kumar J, Bhaskar T. Slow pyrolysis of Defatted Seeds Cakes of African star apple and silk cotton for production of bio-oil. Renew Energy 2020;146:1710–1716. [Crossref]

[37] Chilla V, Suranani S. Thermogravimetric and kinetic analysis of orange peel using isoconversional methods. Mater Today Proc 2023;72:104–109. [Crossref]

[38] Vyazovkin S, Burnham AK, Criado JM, Pérez-Maqueda LA, Popescu C, Sbirrazzuoli N. ICTAC Kinetics Committee recommendations for performing kinetic computations on thermal analysis data. Thermochim Acta 2011;520:1–19. [Crossref]

[39] Chaudhuri P, Pande R, Baraiya NA. A novel insight into the influence of temperature and heating rate on bamboo pyrolysis through kinetics and thermodynamic parameter analysis using thermogravimetric analyser. J Therm. Anal Calorim. 2024;149:1385–1401. [Crossref]